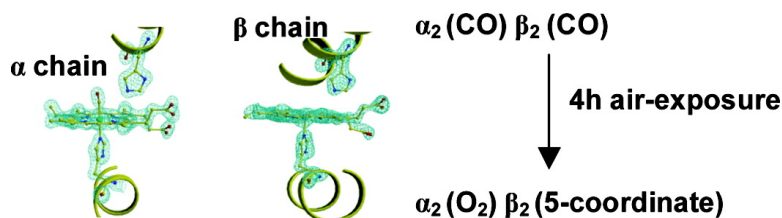


Spectroscopic and Crystallographic Characterization of a Tetrameric Hemoglobin Oxidation Reveals Structural Features of the Functional Intermediate Relaxed/Tense State

Luigi Vitagliano, Alessandro Vergara, Giovanna Bonomi, Antonello Merlino, Cinzia Verde, Guido di Prisco, Barry D. Howes, Giulietta Smulevich, and Lelio Mazzarella

J. Am. Chem. Soc., **2008**, 130 (32), 10527-10535 • DOI: 10.1021/ja803363p • Publication Date (Web): 22 July 2008

Downloaded from <http://pubs.acs.org> on February 8, 2009



More About This Article

Additional resources and features associated with this article are available within the HTML version:

- Supporting Information
- Access to high resolution figures
- Links to articles and content related to this article
- Copyright permission to reproduce figures and/or text from this article

[View the Full Text HTML](#)

Spectroscopic and Crystallographic Characterization of a Tetrameric Hemoglobin Oxidation Reveals Structural Features of the Functional Intermediate Relaxed/Tense State

Luigi Vitagliano,[†] Alessandro Vergara,^{†,‡} Giovanna Bonomi,[‡] Antonello Merlino,[‡]
Cinzia Verde,[§] Guido di Prisco,[§] Barry D. Howes,^{||} Giulietta Smulevich,^{||} and
Lelio Mazzarella^{*,†,‡}

Istituto di Biostrutture e Bioimmagini, CNR, Via Mezzocannone 16, I-80134 Naples, Italy, Department of Chemistry, University of Naples "Federico II", Complesso Universitario Monte S. Angelo, Via Cinthia, I-80126 Naples, Italy, Institute of Protein Biochemistry, CNR, Via Pietro Castellino 111, I-80131 Naples, Italy, and Department of Chemistry, University of Florence, Via della Lastruccia 3, I-50019 Sesto Fiorentino (FI), Italy

Received December 7, 2007; E-mail: lelio.mazzarella@unina.it

Abstract: Tetrameric hemoglobins represent the most commonly used model for the description of the basic concepts of protein allostery. The classical stereochemical model assumes a concerted transition of the protein, upon oxygen release, from the relaxed (R) to the tense (T) state. Despite the large amount of data accumulated on the end-points of the transition, scarce structural information is available on the intermediate species along the pathway. Here we report a spectroscopic characterization of the autoxidation process of the *Trematomus newnesi* major Hb component and the atomic resolution structure (1.25 Å) of an intermediate form along the pathway characterized by a different binding and oxidation state of the α and β chains. In contrast to the α -heme iron, which binds a CO molecule, the β iron displays a pentacoordinated oxidized state, which is rare in tetrameric hemoglobins. Interestingly, the information provided by the present analysis is not limited to the characterization of the peculiar oxidation process of Antarctic fish hemoglobins. Indeed, this structure represents the most detailed snapshot of hemoglobin allosteric transition hitherto achieved. Upon ligand release at the β heme, a cascade of structural events is observed. Notably, several structural features of the tertiary structure of the α and β chains closely resemble those typically observed in the deoxygenated state. The overall quaternary structure also becomes intermediate between the R and the T state. The analysis of the alterations induced by the ligand release provides a clear picture of the temporal sequence of the events associated with the transition. The implications of the present findings have also been discussed in the wider context of tetrameric Hbs.

Introduction

Cellular life relies on rapid and efficient responses to external conditions. The basic molecular events associated with these processes are the structural transitions of the proteins involved. Therefore, a deep understanding of the structural bases of protein allostery is of paramount importance to characterize these processes at the atomic level.^{1–3}

Tetrameric hemoglobins (Hbs) deserve a special position in this field since they are commonly used in biochemistry textbooks to describe the basic concepts of protein allostery.^{3–8}

The pioneering achievements of Perutz led to the identification of two distinct Hb structures: the T (tense) and the R (relaxed) state associated with the deoxygenated and the oxygenated form of the protein, respectively.⁹ On this basis, a stereochemical model for the allosteric transition was proposed. Although Perutz's overall view of Hb allosteric transition is still accepted, more recent crystallographic analyses have clearly shown that tetrameric Hbs possess a larger repertoire of structural states.^{10–19}

[†] Istituto di Biostrutture e Bioimmagini.

[‡] University of Naples.

[§] Institute of Protein Biochemistry.

^{||} University of Florence.

(1) Swain, J. F.; Gierasch, L. M. *Curr. Opin. Struct. Biol.* **2006**, *16*, 102–108.

(2) Gunasekaran, K.; Ma, B.; Nussinov, R. *Proteins* **2004**, *57*, 433–443.

(3) Kuriyan, J.; Eisenberg, D. *Nature* **2007**, *450*, 983–990.

(4) Eaton, W. A.; Henry, E. R.; Hofrichter, J.; Mozzarelli, A. *Nat. Struct. Biol.* **1999**, *6*, 351–358.

(5) Bellelli, A.; Brunori, M.; Miele, A. E.; Panetta, G.; Vallone, B. *Curr. Protein Pept. Sci.* **2006**, *7*, 17–45.

(6) Yonetani, T.; Tsuneshige, A. *C. R. Biol.* **2003**, *326*, 523–532.

(7) Barrick, D.; Ho, N. T.; Simplaceanu, V.; Dahlquist, F. W.; Ho, C. *Nat. Struct. Biol.* **1997**, *4*, 78–83.

(8) Perutz, M. F.; Wilkinson, A. J.; Paoli, M.; Dodson, G. G. *Annu. Rev. Biophys. Biomol. Struct.* **1998**, *27*, 1–34.

(9) Perutz, M. F. *Nature* **1970**, *228*, 726–739.

(10) Safo, M. K.; Abraham, D. J. *Biochemistry* **2005**, *44*, 8347–8359.

(11) Tame, J. R. *Trends Biochem. Sci.* **1999**, *24*, 372–377.

(12) Silva, M. M.; Rogers, P. H.; Arnone, A. *J. Biol. Chem.* **1992**, *267*, 17248–17256.

(13) Srinivasan, R.; Rose, G. D. *Proc. Natl. Acad. Sci. U.S.A.* **1994**, *91*, 11113–11117.

(14) Sutherland-Smith, A. J.; Baker, H. M.; Hofmann, O. M.; Brittain, T.; Baker, E. N. *J. Mol. Biol.* **1998**, *280*, 475–484.

(15) Safo, M. K.; Abraham, D. J. *Protein Sci.* **2001**, *10*, 1091–1099.

(16) Mueser, T. C.; Rogers, P. H.; Arnone, A. *Biochemistry* **2000**, *39*, 15353–15364.

Indeed, novel tense and relaxed structures have been identified and characterized. In spite of the significant amount of data accumulated for the end-points of the transition,^{10,20} structural information on the intermediate forms of the process is still rather limited. Although some interesting features of these states have been unveiled using a variety of techniques,^{21–26} three-dimensional atomic models are not available.

In recent years, time-resolved crystallography has been used to obtain insight into the conformational transitions associated with oxygen binding for several heme proteins.^{27–30} However, these approaches intrinsically suffer from the limitations linked to the compatibility of the conformational transitions monitored with the crystal packing. The large structural variations associated with the R/T transition of tetrameric Hbs likely prevent the use of straightforward time-resolved crystallography techniques for monitoring quaternary structure transitions. Indeed, combined crystallographic and spectroscopic studies on tetrameric Hbs, although remarkable,³¹ have been limited to the initial stages of the tertiary structure transition coupled with oxygen dissociation.

We have recently discovered that Antarctic fish Hbs (AF-Hbs), although structurally and functionally analogous to mammalian Hbs, follow a peculiar oxidation pathway when exposed to air or treated with chemical agents.^{32–34} Intriguingly, the α and β chains of these proteins undergo distinct oxidation processes.³² Particularly unusual is the strong tendency of the β chains to form hexacoordinated bis-histidyl adducts.³³ This state, atypical in folded tetrameric Hbs, is achieved through a severe distortion of the heme pocket. The crystal structures of

these intermediates along the oxidation/unfolding process of AF-Hbs have also revealed that the perturbation at the heme pocket leads to a variation of the quaternary structure which becomes intermediate between the R and the T state. Although these data provided indications on possible structural features of R/T intermediates, their functional implications were limited by the consideration that the quaternary structure variation was induced by the formation of the bis-histidyl complex at the β heme.³³ It is unlikely that such events can play a role in the physiological R→T transition.

In our ongoing research activities aimed at the identification of intermediate species along the oxidation pathway of the major Hb component (Hb1Tn) of the Antarctic fish *T. newnesi*, we determined the nearly atomic resolution crystal structure of a new oxidized form of the protein, which is characterized by distinct binding and oxidation states of the α and β chains. The structural and spectroscopic characterization of this novel species, which precedes the formation of the bis-histidyl complex in the oxidation pathway, provides detailed information on the oxidation process as well as on the mechanism of the allosteric regulation of tetrameric Hbs.

Experimental Section

Crystallization and Data Collection. The carbonmonoxy derivative of Hb1Tn (Hb1TnCO), prepared as previously described,³⁵ was used as the initial state of the air-induced oxidation of the protein. The form characterized in the present investigation was obtained by exposing Hb1TnCO to air for 5 h. To prevent any further oxidation, crystallization experiments were carried out using free-liquid diffusion techniques, by mixing the protein with precipitating agents and buffers in a sealed capillary under CO atmosphere. The crystallization trials were conducted by optimizing the conditions used to crystallize the partial bis-histidyl complex of Hb1Tn (Hb1TnBis).³⁶ Crystals suitable for X-ray diffraction analyses grew in a week by using a protein concentration of 1.5 mg/mL and 14% w/v MPEG5000 in a 50 mM Tris-HCl buffer (pH 7.6).

Diffraction data used in the structural analysis were obtained at 100 K at the ID14–1 beam-line of ESRF (Grenoble, France), using 18% v/v ethylene glycol as cryoprotectant. Diffraction data were processed using the program suite Denzo and Scalepack.³⁷ A summary of the indicators commonly used to estimate the quality of data sets is given in Table 1.

Structure Refinement. The structure of Hb1Tn in its early oxidized form was solved by molecular replacement using the program AMoRe³⁸ and the structure of Hb1TnCO (Protein Data Bank code 1TIN)³⁹ as starting model. The structure was refined using the program SHELX-L.⁴⁰ Each refinement run was followed by manual intervention using the molecular graphic program O.⁴¹ In the final stages of the procedure, the ordered regions of the protein were refined anisotropically.

Inspection of the heme regions revealed two different binding states at the α and β chains. At the α -heme, electron density

- (17) Schumacher, M. A.; Zheleznova, E. E.; Poundstone, K. S.; Kluger, R.; Jones, R. T.; Brennan, R. G. *Proc. Natl. Acad. Sci. U.S.A.* **1997**, *94*, 7841–7844.
- (18) Schumacher, M. A.; Dixon, M. M.; Kluger, R.; Jones, R. T.; Brennan, R. G. *Nature* **1995**, *375*, 84–87.
- (19) Kavanaugh, J. S.; Rogers, P. H.; Arnone, A. *Biochemistry* **2005**, *44*, 6101–6121.
- (20) Park, S. Y.; Yokoyama, T.; Shibayama, N.; Shiro, Y.; Tame, J. R. *J. Mol. Biol.* **2006**, *360*, 690–701.
- (21) Viappiani, C.; Bettati, S.; Bruno, S.; Ronda, L.; Abbuzzetti, S.; Mozzarelli, A.; Eaton, W. A. *Proc. Natl. Acad. Sci. U.S.A.* **2004**, *101*, 14414–14419.
- (22) Englander, J. J.; Del Mar, C.; Li, W.; Englander, S. W.; Kim, J. S.; Stranz, D. D.; Hamuro, Y.; Woods, V. L., Jr. *Proc. Natl. Acad. Sci. U.S.A.* **2003**, *100*, 7057–7062.
- (23) Balakrishnan, G.; Case, M. A.; Pevsner, A.; Zhao, X.; Tengroth, C.; McLendon, G. L.; Spiro, T. G. *J. Mol. Biol.* **2004**, *340*, 843–856.
- (24) Jayaraman, V.; Rodgers, K. R.; Mukerji, I.; Spiro, T. G. *Science* **1995**, *269*, 1843–1848.
- (25) Eaton, W. A.; Henry, E. R.; Hofrichter, J. *Proc. Natl. Acad. Sci. U.S.A.* **1991**, *88*, 4472–4475.
- (26) Lukin, J. A.; Kontaxis, G.; Simplaceanu, V.; Yuan, Y.; Bax, A.; Ho, C. *Proc. Natl. Acad. Sci. U.S.A.* **2003**, *100*, 517–520.
- (27) Knapp, J. E.; Pahl, R.; Srajer, V.; Royer, W. E., Jr. *Proc. Natl. Acad. Sci. U.S.A.* **2006**, *103*, 7649–7654.
- (28) Bourgeois, D.; Vallone, B.; Arcovito, A.; Sciara, G.; Schotte, F.; Anfirud, P. A.; Brunori, M. *Proc. Natl. Acad. Sci. U.S.A.* **2006**, *103*, 4924–4929.
- (29) Schmidt, M.; Nienhaus, K.; Pahl, R.; Krasselt, A.; Anderson, S.; Parak, F.; Nienhaus, G. U.; Srajer, V. *Proc. Natl. Acad. Sci. U.S.A.* **2005**, *102*, 11704–11709.
- (30) Ostermann, A.; Waschkipky, R.; Parak, F. G.; Nienhaus, G. U. *Nature* **2000**, *404*, 205–208.
- (31) Adachi, S.; Park, S. Y.; Tame, J. R.; Shiro, Y.; Shibayama, N. *Proc. Natl. Acad. Sci. U.S.A.* **2003**, *100*, 7039–7044.
- (32) Vitagliano, L.; Bonomi, G.; Riccio, A.; di Prisco, G.; Smulevich, G.; Mazzarella, L. *Eur. J. Biochem.* **2004**, *271*, 1651–1659.
- (33) Riccio, A.; Vitagliano, L.; di Prisco, G.; Zagari, A.; Mazzarella, L. *Proc. Natl. Acad. Sci. U.S.A.* **2002**, *99*, 9801–9806.
- (34) Vergara, A.; Franzese, M.; Merlino, A.; Vitagliano, L.; Verde, C.; di Prisco, G.; Lee, H. C.; Peisach, J.; Mazzarella, L. *Biophys. J.* **2007**, *93*, 2822–2829.

- (35) D'Avino, R.; Caruso, C.; Tamburrini, M.; Romano, M.; Rutigliano, B.; Polverino de Laureto, P.; Camardella, L.; Carratore, V.; di Prisco, G. *J. Biol. Chem.* **1994**, *269*, 9675–9681.
- (36) Riccio, A.; Vitagliano, L.; di Prisco, G.; Zagari, A.; Mazzarella, L. *Acta Crystallogr., Sect. D: Biol. Crystallogr.* **2001**, *D57*, 1144–1146.
- (37) Otwinowsky, Z.; Minor, W. *Methods Enzymol.* **1997**, *276*, 307–326.
- (38) Navaza, J. *Acta Crystallogr., Sect. A: Found. Crystallogr.* **1994**, *A50*, 157–163.
- (39) Mazzarella, L.; D'Avino, R.; di Prisco, G.; Savino, C.; Vitagliano, L.; Moody, P. C.; Zagari, A. *J. Mol. Biol.* **1999**, *287*, 897–906.
- (40) Sheldrick, G. M.; Schneider, T. R. *Methods Enzymol.* **1997**, *277*, 319–343.
- (41) Jones, T. A.; Zou, J. Y.; Cowan, S. W.; Kjeldgaard, M. *Acta Crystallogr., Sect. A: Found. Crystallogr.* **1991**, *47*, 110–119.

Table 1. Crystal Data, Data Collection, and Refinement Statistics

Crystal Data and Data Collection Statistics	
space group	C2
cell parameters	
a (Å), b (Å), c (Å), β (deg)	88.46, 87.66, 55.50, 99.2
resolution range (Å)	30.0–1.25
asymmetric unit content	$\alpha\beta$ dimer
number of observations	470758
number of unique reflections	114368
completeness (%)	99.6 (99.4) ^a
redundancy	4.1
R_{merge}	0.030 (0.332) ^a
Refinement Statistics	
resolution range (Å)	30.0–1.25
$R_{\text{factor}}/R_{\text{free}}$	16.7/20.2
number of protein atoms	2363
number of water molecules	296
root mean square deviations from ideality	
1–2 distances (Å)	0.019
1–3 distances (Å)	0.038

^aThe value in parentheses refers to the highest resolution shell (1.29–1.25 Å).

corresponding to the CO ligand was clearly observed, whereas density at the β iron suggested that the ligand was released (see Results).

The final model of Hb α (CO) β (penta) has been refined at an R_{factor} of 0.167 (R_{free} 0.202) by using diffraction data extending up to 1.25 Å resolution. The stereochemistry of the final model, checked using the program PROCHECK,⁴² is in line with that exhibited by protein structures refined at high resolution. The atomic coordinates of this Hb1Tn α (CO) β (penta) were deposited in the PDB (code 3D1K).

Sample Preparations for Spectroscopy Experiments. The Hb1TnCO sample used in the autoxidation process was prepared by exposing ferrous Hb1Tn to CO in sealed Raman cells. For comparative purposes, also the deoxy, the oxy, and the fully oxidized forms of the protein were prepared. In particular, the oxidized Met-Hb derivatives were prepared by treating the protein with an excess of potassium hexacyanoferrate(III). A gel filtration experiment on a Biogel P-6DG column equilibrated with Tris-HCl pH 7.5 was performed to remove the oxidant. The deoxy samples were prepared by adding 2–3 mL of sodium dithionite (20 mg/ml) to 50 mL of deoxygenated buffered solution of Met-Hb. The oxy sample was prepared by gel filtration of a deoxy sample on a Biogel P-6DG column equilibrated with Tris-HCl pH 7.5.

Spectroscopy. The autoxidation of ferrous carbonmonoxy Hb1Tn in solution was followed by resonance Raman (RR) and electronic absorption spectroscopy by exposing the protein solution to air. The room temperature RR and electronic absorption experiments were carried out on protein samples in 50 mM Tris-HCl (pH 7.5) placed in NMR tubes (0.4 cm optical path). The heme concentration of Hb1Tn samples was 10 μ M. The sample preparation procedures are described in Supporting Information.

Electronic absorption spectra were measured with a double-beam Cary 5 spectrophotometer (Varian, Palo Alto, CA). The RR spectra were obtained by excitation with the 413.1 nm line of a Kr⁺ laser (Coherent, Innova 300 C, Santa Clara, CA) and the 441.6 nm line of a HeCd laser (Kimmon IK4121R-G) as previously reported.⁴³

The RR spectra were calibrated with indene, dimethyl sulfoxide (DMSO), pyridine, and CCl₄ as standards to an accuracy of ± 1 cm⁻¹ for intense isolated bands. Curve fitting was carried out using

a program (Lab Calc, Galactic) to simulate the spectra using a Lorentzian line shape.

Results

Overall Quality of the Structure of the Novel Intermediate State in Hb1Tn Oxidation Pathway. With the aim of characterizing intermediate species along the oxidation pathway of the major Hb component of *T. newnesi*, crystallization experiments were conducted in a CO atmosphere on protein samples of the carbonmonoxy derivative of Hb1Tn previously exposed to air for about 5 h. Although some heterogeneity in the starting protein samples was expected, crystallization trials yielded crystals with a good morphology and excellent diffraction quality (resolution limit 1.25 Å). Interestingly, the crystals grown for this novel form are isomorphous to those obtained for the carbonmonoxy form³⁹ and for the partial hemichrome state³³ of Hb1Tn. This observation ensures that the structural modifications herewith described represent a molecular property of the protein. The analysis of the resulting electron density maps indicates that it is extremely well-defined for most of the protein residues. Representative examples of maps of key regions of the protein are shown in Figures 1 and S1. A single disordered region (CD β), few solvent-exposed lysyl residues and C-terminal His β 145 exhibit poor electron density.

Heme States. Inspection of the electron density maps clearly indicated that the binding state of the heme iron of the α and β chains was different. The electron density of the α -heme region provides convincing evidence that a diatomic ligand is bound to the iron (Figure 1A). Although some Hb1Tn oxygenation likely occurs upon air-exposure (see also below), the CO atmosphere inside the capillary used for crystallization and the very high affinity of tetrameric Hbs for this ligand suggest that a CO molecule is bound to this heme iron. As usually found in Hb carbonmonoxy derivatives, the iron is located in the plane of the porphyrin ring. The electron density is also very well-defined for all residues of the heme pocket. No significant difference was detected by comparing ligand binding at the α -heme region of the present structure with that of Hb1TnCO.³⁹

A radically different picture emerges from the analysis of the electron density maps of the β -heme region (Figure 1B). Indeed, no electron density is present at the ligand binding site when it is countered at 4.1 σ . If the level of the electron density is decreased, a small peak appears at 2.7 Å from the iron (Figure 1B). The shape of this weak electron density peak is not compatible, even when visualized at very low levels, with a low-occupancy diatomic ligand. On the other hand, refinement indicates that a water molecule with a partial occupancy (0.6) is compatible with the density. This water molecule could also establish an hydrogen bond with the N ϵ^2 atom of the distal histidine residue, although this interaction is characterized by a nonoptimal geometry (distance 3.14 Å and a donor-hydrogen-acceptor angle of $\sim 125^\circ$). The absence of a diatomic ligand on the β -heme iron suggests that the 5 h air exposure of Hb1Tn has led to oxidation of the β iron. Indeed, binding of the CO ligand to a hypothetical iron(II) would have been expected in the CO atmosphere of the crystallization experiments. This suggestion is corroborated by the observation that the β iron does not exhibit the displacement from the heme plane typically found in deoxygenated iron(II) Hbs. Hence, the crystallographic data suggest that Fe(III) is the dominant species at the β heme in the crystal and that in a fraction of molecules a water molecule weakly interacts with the iron. The location of the water molecule and its interaction with the iron is very different from

(42) Laskowski, R. A.; MacArthur, M. W.; Moss, M. D.; Thornton, J. M. *J. Appl. Crystallogr.* **1993**, *26*, 283–291.

(43) Droghetti, E.; Howes, B. D.; Feis, A.; Dominici, P.; Fittipaldi, M.; Smulevich, G. *J. Inorg. Biochem.* **2007**, *101*, 1812–1819.

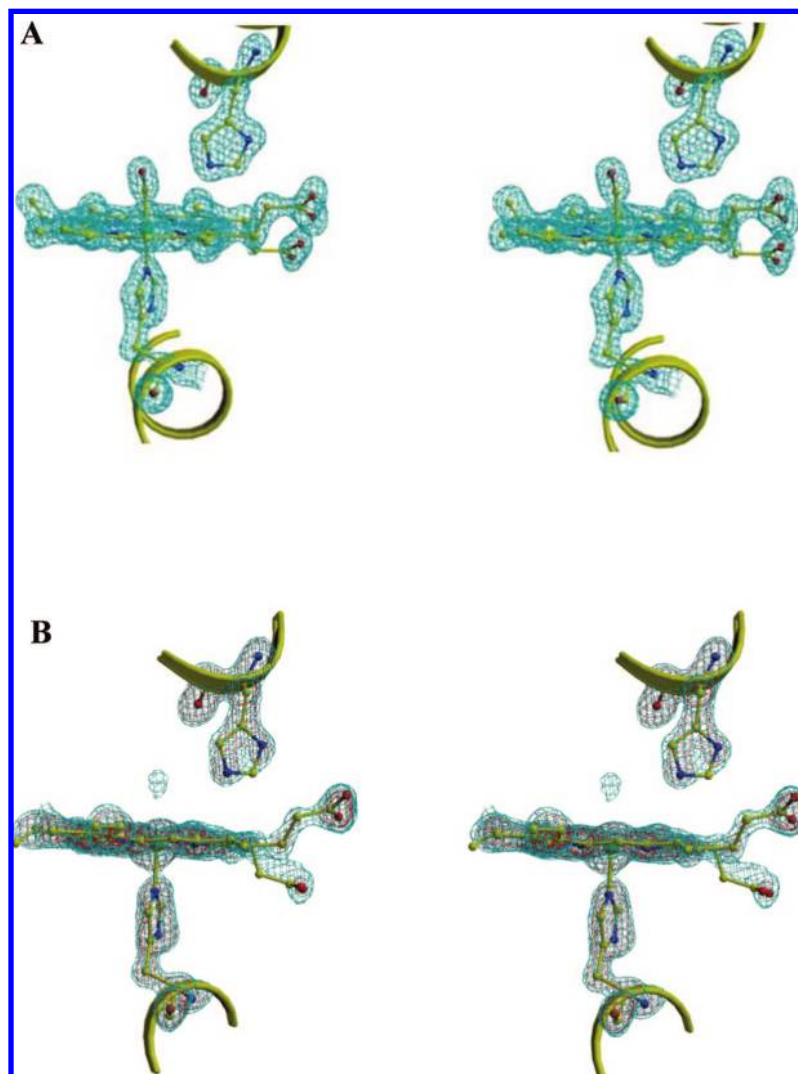


Figure 1. Stereodiagrams of the omit ($F_o - F_c$) electron density maps of α (A) and β (B) heme regions. The α -heme map has been contoured at 3.0σ , whereas electron densities at the β heme are contoured at 4.1σ (red) and 3.0σ (cyan).

that observed in mammalian Hb aquomet states, which are characterized by Fe–water distance of ~ 2.1 Å. Since the electron density is very well-defined for the vast majority of the protein residues, the presence of the water molecule does not have any impact either on the local or the overall Hb1Tn structure. It is worth mentioning that this partially occupied water molecule has been systematically reproduced in all data collections conducted on crystals grown from Hb1Tn exposed to air for a few hours.

In order to obtain further clues on this issue, the oxidation pathway of Hb1Tn, through air-exposure of protein solutions, was followed by RR and electronic absorption spectroscopy. The high frequency region (1300 – 1700 cm^{-1}) of the RR spectrum includes the porphyrin in-plane vibrational modes, that are sensitive to the electron density of the macrocycle, the oxidation, coordination, and spin state of the iron atom.⁴⁴ The spectra of Hb1TnCO in the high-frequency region upon air-exposure are reported in Figure 2A. As expected, the RR spectrum of the starting state is characterized by marker bands of the carbonmonoxy form (e.g., ν_3 1501 cm^{-1} and ν_2 1584 cm^{-1}). The weak bands at 1470 cm^{-1} (ν_3) and 1355 cm^{-1} (ν_4) (data not shown) are due to the deoxy form produced by laser-induced photolysis of the CO ligand. In the RR low frequency

region the band at 502 cm^{-1} , not present in the spectrum of the deoxy form (data not shown), is assigned to the Fe–CO stretching mode (Figure S2).

The weak charge transfer (CT1) band at 630 nm observed during the early stages of air-exposure in the absorption spectrum (1–2 h) (Figure 2B, trace 2) is consistent with the immediate appearance of an aquo hexacoordinated high spin (6cHS) ferric species. Longer air exposure times (3–4 h) lead to the progressive replacement of the CO ligand by an O_2 ligand. This is clearly evident from the upshift of the α/β bands and downshift of the Soret band (trace 3, Figure 2B and 2C) to values typical of the oxy form. Accordingly, the ν_3 band upshifts to 1504 cm^{-1} and the ν_{10} at 1639 cm^{-1} intensifies (Figure 2A, trace 3). A shoulder at 1479 cm^{-1} can also now be observed, consistent with the increased presence of the 6cHS form. In addition, the intensity of the $\nu_{\text{Fe-CO}}$ band at 502 cm^{-1} decreases (data not shown). After 3–4 h air exposure times, in all the UV–vis spectra (Figure 2B, traces 3, final), a weak band at about 660 nm appears whose origin remains unclear.

(44) Spiro, T. G. *Adv. Protein Chem.* **1985**, *37*, 111–159.

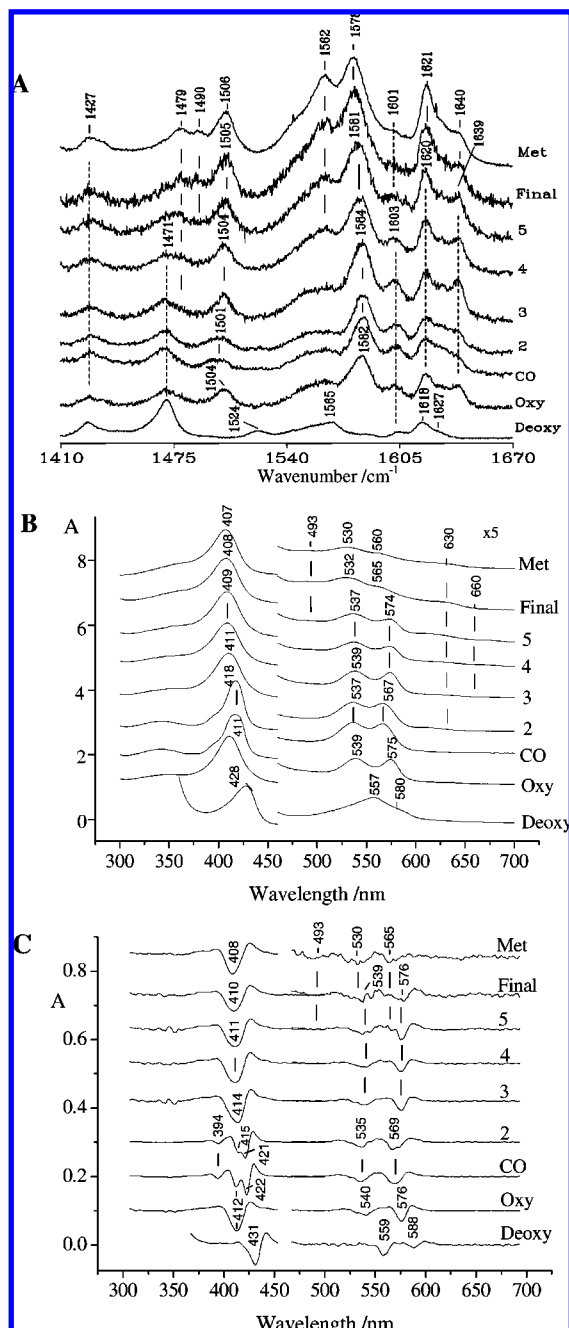


Figure 2. The autoxidation of 10 μM Hb1TnCO in 50 mM Tris-HCl pH 7.5 followed by resonance Raman (A), electronic absorption (B), and its second derivative (C) spectroscopy. (A) Experimental conditions RR spectra: 413.1 nm excitation wavelength, 1 cm^{-1} spectral resolution; (deoxy) 10 mW laser power at the sample, average of two spectra with 10 min integration time; (oxy) 1 mW laser power at the sample, average of four spectra with 10 min integration time; (CO and trace 2) 0.1 mW laser power at the sample, average of six spectra with 10 min integration time; (traces 3 and 4) 0.1 mW laser power at the sample, average of five spectra with 10 min integration time; (trace 5 and final) 0.1 mW laser power at the sample, average of three spectra with 10 min integration time; (Met) 11 mW laser power at the sample, 5 min integration time. The intensities are normalized to that of the ν_4 band. (B and C) Absorption and second derivative spectra, respectively, of the deoxy, oxy, CO, met forms, and autoxidation of the CO form (traces 2–5 and final). The 460–700 nm region is expanded 5-fold. The ordinate scale refers to the absorbance of the deoxy spectrum. The spectra have been shifted along the ordinate axis to allow better visualization. The autoxidation times of the traces are: trace 2, 2 h; trace 3, 4 h; trace 4, 7 h; trace 5, 10 h; final, 12 h.

Subsequent spectra (4–10 h) reveal the broadening of the bands at 537 and 574 nm in the absorption spectrum (Figure 2B, trace 4), the presence of a weak component at 565 nm in the second derivative spectrum (Figure 2C, trace 5), and frequency shifts of the ν_3 and ν_2 bands to 1505 and 1581 cm^{-1} , respectively (Figure 2A, trace 5). These changes are consistent with the formation of a low spin hexacoordinated bis-histidine (6cLS) (hemichrome) species. A new ν_3 band at 1490 cm^{-1} , characteristic of a high spin pentacoordinated (5cHS) ferric form, also becomes evident in this time interval (Figure 2A, trace 5). It should be noted that the order of appearance of the 5cHS and 6cLS species is not completely clear as the only signature for the presence of the 5cHS, which is not obscured by other more intense bands, is the ν_3 band at 1490 cm^{-1} . Nevertheless, the crystallographic observation suggests that the 5cHS state precedes the 6cLS state at the β heme. Moreover, it is important to note that the simultaneous presence in the RR spectrum of the band at 1490 cm^{-1} together with those due to the oxy form demonstrate that the 5cHS ferric and the oxy forms coexist under these conditions. Furthermore, the red-shift of the α/β bands compared to the Met form (obtained by oxidation with potassium ferricyanide) (Figure 2B) indicates that the oxy species persists even in the sample exposed to air for 12 h (denoted as final in Figure 2). This is particularly clear in the second derivative presentation of the visible region of absorption spectra (Figure 2C), where components corresponding to the oxy form (at 539 and 576 nm) are observed together with components from the bis-histidine LS form (at 530 and 565 nm). Similar features were observed in the final spectra for the autoxidation of other Hb1TnCO samples for oxidation times up to 22 h (data not shown). The final spectrum corresponds to the point in the oxidation pathway when the RR and absorption spectra showed no significant further changes for more than 2 h.

The Met form obtained by chemical oxidation (Figure 2A) is characterized by three ferric species, i.e. 5cHS, (bis-histidine) 6cLS, and (aquo) 6cHS, whereas the deoxy RR spectrum is a pure 5cHS form (ν_3 at 1471 cm^{-1}) with the Fe-His stretching frequency about 7 cm^{-1} lower than that for myoglobin (Figure S2).⁴⁵ An analysis of the vinyl stretching modes is reported in Supporting Information (Figure S3).

The spectroscopic data clearly indicate that the oxidation process of Hb1Tn proceeds through a variety of different forms. Intriguingly, the spectra detected at 4–10 h correspond to the state whose structure has been here determined, namely the formation of a pentacoordinated species. The CO atmosphere used for the crystallization form has led to the replacement of the oxy with the carbonmonoxy form.

Tertiary and Quaternary Structure. The analysis of the binding state of the α and β heme iron atoms clearly indicates that the protein characterized in the present study, hereafter denoted as Hb1Tn α (CO) β (penta), is a partially ligated tetrameric Hb. This provides the opportunity to investigate the local and the overall structure of the protein in these unusual conditions. In particular, the structure of Hb1Tn α (CO) β (penta) was analyzed in comparison with the carbonmonoxy derivative (Hb1TnCO)³⁹ and with the fully oxidized species (Hb1TnBis) of Hb1Tn.³³ In the absence of structural data on the deoxygen-

(45) Kitagawa, T.; Nagai, K.; Tsubaki, M. *FEBS Lett.* **1979**, *104*, 376–378.

ated form of Hb1Tn,³⁶ the deoxy structure of the closely related Hb isolated from *Trematomus bernacchii* [HbTb(deoxy)]⁴⁶ was considered.

The comparison of the overall rmsd values of the individual chains (Table S1 Supporting Information) indicates that the Hb1Tn α (CO) β (penta) α chain is slightly closer to the corresponding subunit of Hb1TnCO than to the HbTb(deoxy) α chain (0.52 versus 0.65 Å). Conversely, the Hb1Tn α (CO) β (penta) β chain is closer to HbTb(deoxy) than to Hb1TnCO (0.44 versus 0.56 Å). This finding indicates that the similarity of the binding state is reflected in the overall similarity of the individual subunits.

The analysis of the variations induced by ligand release at the β heme indicates that this release produces a significant rearrangement of the heme pocket. As shown in Figure S4 the mutual orientation of the E and F helices changes. In particular, a scissoring-like motion of the EF corner is observed. Indeed, the C α –C α distance between the proximal and distal His changes from 14.4 (Hb1TnCO) to 13.9 Å (Hb1Tn α (CO) β (penta)). In agreement with a previous investigation,³³ a statistical analysis carried out on 404 β chains of vertebrate Hbs reported in the PDB indicates that the value of this distance is quite constant, irrespective of whether the structure is R or T. Indeed, for most of the structures the differences are confined within 0.3 Å (Figure S5A). The value observed for this distance in Hb1Tn α (CO) β (penta) (13.9 Å) falls on the lower limit of the distribution. To obtain a rough estimate of the energy required for the EF scissoring motion we converted the distribution of the distances into energies by using the Boltzmann equation (Figure S5B). Our analysis suggests that the energy required to compress the EF region to the extent observed in Hb1Tn α (CO) β (penta) corresponds to 7–8 kcal/mol (Figure S5B). Such a value, although approximate due to the intrinsic limitations of the method applied, indicates that this type of movement is accessible in tetrameric Hbs during their R–T transition. On the other hand, the compression of the EF region upon hemichrome formation (C α –C α distance \sim 12.5 Å) requires several dozens of kcal/mol. Only the formation of the additional covalent bond between the distal His and the heme iron may compensate for this large energetic cost.

A comparison of the overall structure of Hb1Tn α (CO) β (penta) and Hb1TnCO clearly indicates that the structural modification associated with ligand release at the β heme is propagated to the α heme. The absence of an exogenous ligand at the β iron produces a significant displacement of the FG loop and the C helix of the β chain (Figure 3 and Figure S6). These alterations are stabilized and amplified by the insertion of Tyr145 β , which is solvent-exposed and disordered in Hb1TnCO, into the protein region delimited by the heme pocket, the F and G helices, and by the FG corner (Figure 3).

The modifications of the FG corner are transmitted to the CD β region either directly or through the heme (Figure 3 and Figure S6). Since the CD β region is at the $\alpha_1\beta_2$ ($\alpha_2\beta_1$) interface, these variations produce a profound impact on the quaternary structure of the protein. In the structure of Hb1TnCO, Tyr41 β (C β helix) and Tyr42 α (C α helix) are rather distant (OH–OH distance of 4.31 Å) (Figure 3). The displacement of Tyr41 β allows the insertion of Arg40 β , which is solvent-exposed in Hb1TnCO, between the two Tyr. In Hb1Tn α (CO) β (penta), Arg40 β simultaneously binds the side chains of Tyr41 β and

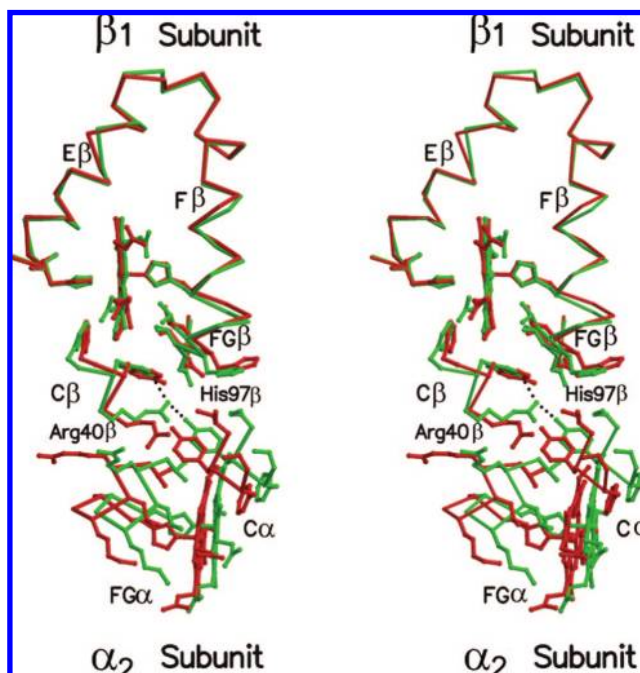


Figure 3. Stereodiagram of the amplification of the modifications induced by the ligand release to the quaternary structure. The C α trace of Hb1Tn α (CO) β (penta) and Hb1TnCO is colored in green and red, respectively. The residues of the entire β chain have been superimposed. The anchoring of Tyr42 α and Tyr41 β side chain by Arg40 β in Hb1Tn α (CO) β (penta) is also shown.

Tyr42 α (Figure 3). This rearrangement is accompanied by a movement of Arg93 α , which covers the cavity filled by Arg40 β and further limits the mobility of this latter residue. As a consequence of these modifications, the position of key residues located at the $\alpha_2\beta_1$ ($\alpha_1\beta_2$) becomes intermediate between those observed in the canonical R and T states. In particular, the relative orientation of the residue His97 β and the helix C of the α chain, which is commonly assumed as a signature of the R or T state of tetrameric Hbs,¹¹ is indicative of this general trend (Figure 4). Similarly, the Asp99 β and Tyr42 α side chains, which form a stabilizing hydrogen bond in the T state, are closer in Hb1Tn α (CO) β (penta) compared to Hb1TnCO (Figure S7).

The overall rearrangement of the $\alpha_2\beta_1$ ($\alpha_1\beta_2$) interface has direct consequences at the α heme region, thus completing the heme–heme communication pathway (Figure 5 and Figure S7). Indeed, as shown in Figure 5, the side chains of Tyr42 α and Tyr141 α are engaged in hydrogen-bonding interactions with the same peptide group (residues 94–95). The structural modifications induced by ligand dissociation at the β heme and amplified at the $\alpha_2\beta_1$ ($\alpha_1\beta_2$) interface lead to a rearrangement of the FG α region. Particularly important is the change of the Tyr141 α side chain conformation, which closely resembles that taken by this residue in the T state.^{20,46,47} The concomitant T-state conformation of Tyr141 α and the presence of the CO ligand at the α heme is indicative of a local strain in Hb1Tn α (CO) β (penta) (Figure 5). Conceivably, the high concentration of CO under the crystallization conditions prevents the ligand dissociation and the complete transition to the T state.

A comparative analysis of the quaternary structure of Hb1Tn in different binding states clearly demonstrates that the transition

(46) Mazzarella, L.; Vergara, A.; Vitagliano, L.; Merlino, A.; Bonomi, G.; Scala, S.; Verde, C.; di Prisco, G. *Proteins* **2006**, *65*, 490–498.

(47) Mazzarella, L.; Bonomi, G.; Lubrano, M. C.; Merlino, A.; Riccio, A.; Vergara, A.; Vitagliano, L.; Verde, C.; di Prisco, G. *Proteins* **2006**, *62*, 316–321.

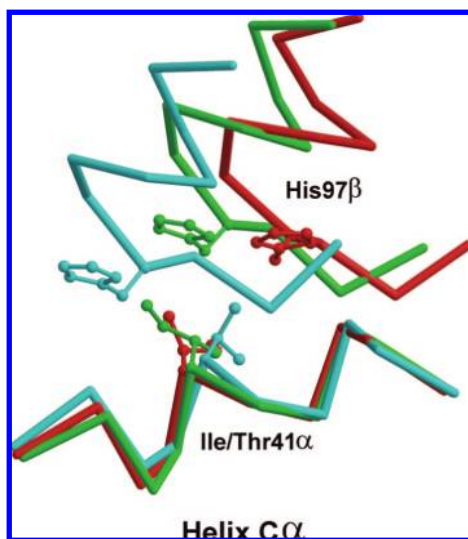


Figure 4. Relative orientation of residue His97 β and the helix C of the α chain. Hb1Tn α (CO) β (penta), Hb1TnCO, and HbTb(deoxy) are colored in green, red, and cyan, respectively. Residue 41 of the α chain is Ile and Thr in Hb1Tn and HbTb sequence, respectively. Residues of the entire α chain have been superimposed.

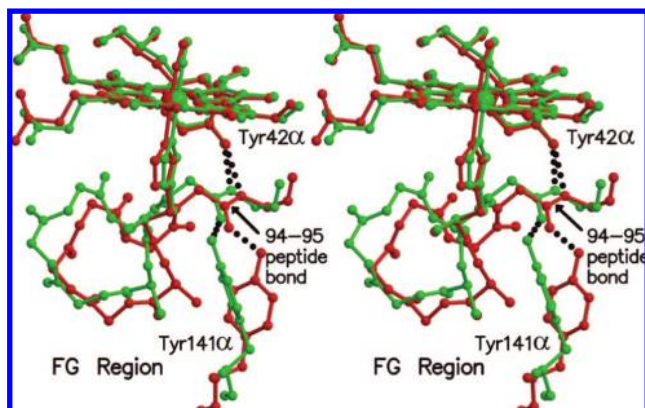


Figure 5. Strain at the α heme produced by ligand dissociation at the β heme. The C α trace of Hb1Tn α (CO) β (penta) and Hb1TnCO is colored in green and red, respectively. The residues of the entire α chain have been superimposed. For the sake of clarity, some side chains have been omitted.

described here falls into the functional R \rightarrow T pathway. Indeed, the stepwise superimposition of $\alpha\beta$ dimers suggests that the optimal fit of $\alpha_2\beta_2$ of Hb1TnCO and Hb1Tn α (CO) β (penta), starting from overlapped $\alpha_1\beta_1$ dimers, requires a rotation of 2.8°. The rotation required for the same transformation between Hb1Tn α (CO) β (penta) and HbTb(deoxy) is -7.8° . The rotation corresponding to the overall R \rightarrow T transition (Hb1TnCO versus HbTb(deoxy)) is -10.5° . Interestingly, the orientation of the rotation axis of Hb1TnCO/HbTb(deoxy), Hb1TnCO/Hb1Tn α (CO) β (penta), and Hb1Tn α (CO) β (penta)/HbTb(deoxy) is remarkably similar, since the spherical coordinate Ψ of the axes is 0° , 5.1° , and 14.8° , respectively.

These findings are corroborated by the analysis of difference distance matrices, that have frequently been used to analyze structural transitions of tetrameric Hbs,^{13,32,48} computed by using the program DDMP (http://www.csb.yale.edu/userguides/datamanip/ddmp/ddmp_descrip.html) and the structures of

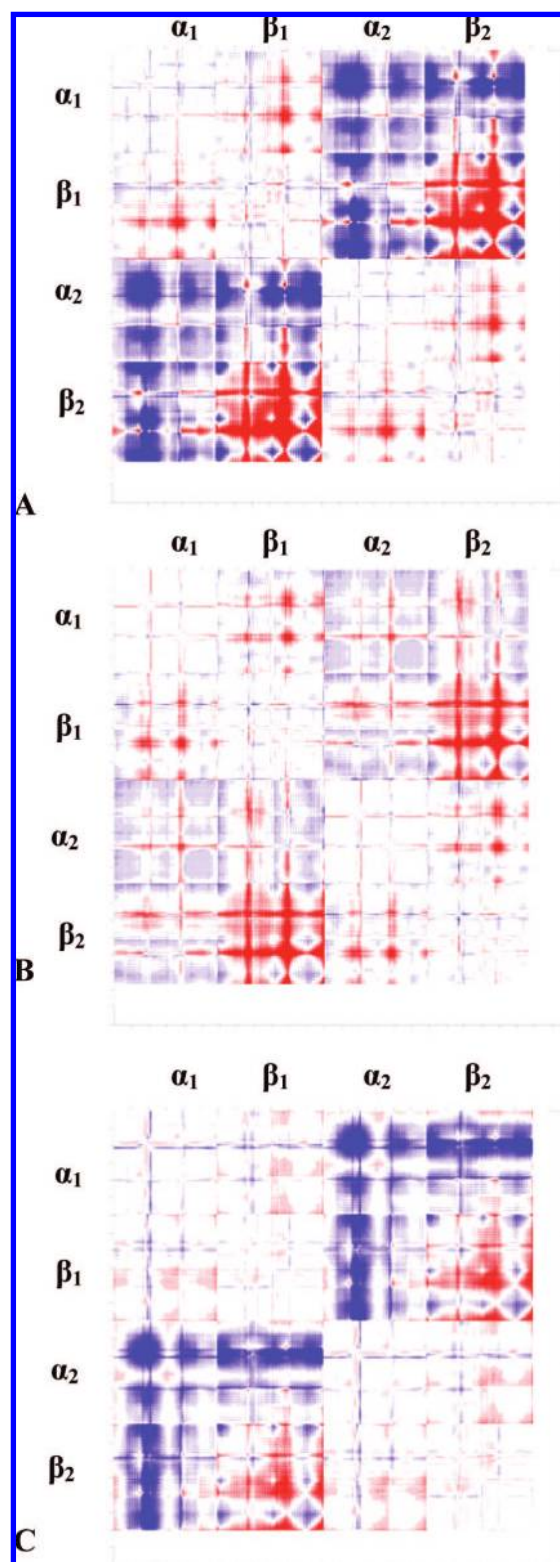


Figure 6. Difference distance matrices of Hb1TnCO vs HbTb(deoxy) (A), Hb1TnCO vs Hb1Tn α (CO) β (penta) (B), and Hb1Tn α (CO) β (penta) vs HbTb(deoxy) (C). In each map, blue regions represent residues that move closer in the second structure, whereas the opposite happens in the red regions. The color range extends from -3.25 Å (dark red) to 3.25 Å (dark blue).

Hb1TnCO, HbTb(deoxy), and Hb1Tn α (CO) β (penta) (Figure 6). As shown in Figure 6, the overall organization of the subunits in Hb1Tn α (CO) β (penta) within the tetramer is intermediate

(48) Wilson, J.; Phillips, K.; Luisi, B. *J. Mol. Biol.* **1996**, *264*, 743–756.

between that found in Hb1TnCO and HbTb(deoxy). Indeed, a comparative analysis of the analogies of the diagrams reported in Figures 6A and 6B clearly indicates that the events linked to the ligand release at the β heme generate some of the structural alterations induced by the R \rightarrow T transition. In particular, most of the structural alterations regarding the relative orientation of the subunits α_1 - α_2 and β_1 - β_2 observed in the R \rightarrow T transition are well reproduced in the conversion of Hb1TnCO to Hb1Tn α (CO) β (penta). These findings clearly indicate that the peculiar location of some key residues at subunit-subunit interfaces of Hb1Tn α (CO) β (penta) is not simply due to structural variations of the local structure but reflects significant modifications of the overall protein structure occurring upon ligand release.

Discussion

The characterization of intermediate structural states involved in biological processes is of considerable importance for elucidating the molecular events involved. However, it often requires the use of non-standard techniques and rarely leads to a detailed characterization of the investigated system. The present structure (Hb1Tn α (CO) β (penta)) represents a fortunate exception to this general trend. Indeed, this quasi-atomic resolution structure provides interesting clues on the oxidation process and on the functional R/T transition of a tetrameric Hb isolated from the Antarctic fish *T. newnesi*. It is important to mention that, although this state was found serendipitously, its formation is easily reproduced, even using Hb1Tn crystals grown under different conditions (2 M ammonium sulfate).

The crystallographic and spectroscopic analyses reported here show that the present structure corresponds to an intermediate α ferrous/ β ferric state along the Hb1Tn oxidation process. Not only do these novel data corroborate the previous finding that in Antarctic fish Hbs (AF-Hbs) α and β chains follow distinct oxidation pathways, but they also provide clear indications that the oxidation of the β iron precedes the oxidation of the α iron. Interestingly, the oxidation of the β iron leads to the formation of a pentacoordinated state which is rarely observed in tetrameric Hbs. Indeed, detection of a pentacoordinated state for these Hbs has been reported only for the cathodic Hb from *T. newnesi*³⁴ and an Arctic fish Hb using EPR.⁴⁹ The present findings, together with the known tendency of AF-Hbs β chains to form bis-histidyl complexes,³² suggest that a variety of different oxidized states are accessible to these subunits. The structure of Hb1Tn α (CO) β (penta) also shows that the pentacoordinated form at the β heme coexists with a state characterized by the presence of a weakly bound water molecule at 2.7 Å. Similar configurations have been occasionally found in peroxidases.⁵⁰ If one recalls that the spectroscopic data indicate the first event in the Hb1Tn oxidation to be the formation of an aquomet (6cHS) form, it is possible that this species corresponds to that with a weakly coordinated water molecule detected in the crystal state.

These results, along with previous literature data,^{32,34,51} provide evidence that AF-Hbs follow oxidation pathways that are distinct from those exhibited by other tetrameric Hbs. Interestingly, the finding that AF-Hbs may assume states, such

as hemichrome and pentacoordinated forms, that are typically associated with Hbs with lower complexity, demonstrates that such states are also accessible to tetrameric Hbs.

The peculiarity of the Hb1Tn oxidation pathway is not limited to the heme species involved. Indeed, the combined analysis of the spectroscopic and structural data also suggests that the oxidation pathways of α and β hemes are intimately related, although they lead to different final states. In this context, spectroscopic data indicate that the early stages of the oxidation process are characterized by the coexistence of iron(II) and iron(III) species. These states evolve, leading to the concomitant formation of aquomet, hemichrome, and pentacoordinated ferric states. A possible structural explanation of these observations may be provided by assuming that hemichrome formation at the β iron is not compatible with the presence of a diatomic ligand, or at least of CO, at the α heme. In this context, it should be noted that the first structure of air-oxidized Hb1Tn, initially interpreted as a α (CO) β (hemichrome) state,³⁰ was reconsidered to be α (O₂) or even a mixture of α (O₂) and α (aquomet).²⁹ In support of such an interpretation, the oxidation process is found to start at the β iron with the formation of the aquomet, that will convert into a pentacoordinated state. This is followed by the oxidation of the α iron to the aquomet state. Finally, the process is completed by the formation of the hemichrome states at the β iron. In this framework, the short air-exposure of the protein sample and the presence of CO during the crystallization has prevented the oxidation of the α iron, thus trapping the peculiar state here characterized. This mechanism is in accord with other experiments conducted on cyanide forms of AF-Hbs (unpublished results). The interplay of the oxidation pathways of α and β chains is an alternative manifestation of the heme-heme communication mechanism typically adopted in the description of the functional R \rightarrow T transition.

Since the functional R \rightarrow T transition and the intricate oxidation process of Hb1Tn are likely two manifestations of the strong heme-heme coupling in Hbs, it is not surprising that the structure of the partially oxidized Hb1Tn provides clues on the structural features of intermediate states in the oxygen binding/release process. Indeed, the oxidation of the β chains leads to an irreversible ligand release which produces a stable symmetric state α (CO) β (deoxy) that mimics an intermediate state of the type H1r1T, according to the notation of Edelstein.⁵² The analysis of the intermediate structure clearly provides a precise structural pathway that connects the release of the ligand from the β iron to the creation of strain at the α iron. The starting event of the process is the scissoring motion of the β EF region that initiates a cascade of structural signals that propagate up to the distant α iron site. The present data also suggest that, in contrast to the structural alterations induced by hemichrome formation,^{32,33} minimal modifications of the EF region, whose structure is highly preserved within tetrameric Hbs, are sufficient to initiate the quaternary structure transition. This is particularly interesting if one considers that R states are by definition relaxed states endowed with structural malleability that, in principle, may dissipate structural signals. In this framework, the EF region, whose structural alterations are strongly limited by the presence of the heme group, can generate events that are transmitted to sites up to \sim 25 Å. An approximate estimate of the energetic cost (7–8 kcal/mol) required for the observed EF compression indicates this state can be easily accessed in the R \rightarrow T transition.

(49) Giordano, D.; Vergara, A.; Lee, H. C.; Peisach, J.; Balestrieri, M.; Mazzarella, L.; Parisi, E.; di Prisco, G.; Verde, C. *Gene* **2007**, *406*, 58–68.

(50) Smulevich, G. *Biospectroscopy* **1998**, *4*, S3–17.

(51) Vergara, A.; Vitagliano, L.; Verde, C.; di Prisco, G.; Mazzarella, L. *Methods Enzymol.* **2008**, *436*, 425–444.

(52) Edelstein, S. J. *J. Mol. Biol.* **1996**, *257*, 737–744.

The present structure provides clear indications on the role played by specific residues located either at the $\alpha_1\beta_2$ ($\alpha_2\beta_1$) interface or in the heme pockets. The interactions established by the conserved residue Arg40 β with Tyr41 β and Tyr42 α are particularly important for the stabilization of this R/T intermediate state. The interaction Tyr41 β -Arg40 β , which is Hb1Tn sequence specific since residue 41 β is Phe in human Hb and His in HbTb, likely contributes to the stability of Hb1Tn α -(CO) β (penta).

Over the years, the identification of the structural features of tetrameric Hb intermediates formed during the R \rightarrow T transition has been extensively pursued. These studies, mainly conducted on mammalian Hbs, have been carried out by adopting diversified approaches based on cross-linked forms, metal hybrid states, complexes with effectors, mutants, liganded T states, and unliganded R states.^{16,18,19,31,48,53–58} The analogies of the structural modifications detected in mammalian and fish Hbs upon the R \rightarrow T transition (Figures 6 and S8A) suggest that the structural features of Hb1Tn α (CO) β (penta) may be shared by intermediate states of the entire class of vertebrate Hbs. Indeed, difference distance matrices indicate that, despite some sequence-

dependent specificities, the state described herein is also intermediate in the framework of human R and T states (Figures S8B and S8C). Interestingly, the structure of Hb1Tn α (CO)- β (penta) is more suggestive of an intermediate state than the mammalian Hb structures previously reported (Figures S8 and S9). Molecular modeling also suggests that the fitting of the human Hb sequence on the structure of Hb1Tn α (CO) β (penta) does not generate any significant steric hindrance. It is also worth mentioning that in close agreement with predictions for human Hb,²⁵ the intermediate state is closer to the R than to the T state.

In conclusion, the crystallographic and spectroscopic characterization of Hb1Tn presented here shows that it is able to assume peculiar oxidation states in native-like conditions that may indicate that the protein is involved in functional redox processes yet to be identified. In addition, our data provide evidence that there is no major steric barrier that prevents a straightforward R \rightarrow T transition.

Acknowledgment. This work was financially supported by PRIN and PNRA (Italian National Programme for Antarctic Research), in the framework of the programme Evolution and Biodiversity in the Antarctic (EBA), and by grants to G. S. from the Università di Firenze (ex 60%). We thank the ESRF Synchrotron (Grenoble, France) for beam-time and the staff of the beam-line ID14-1 for assistance during data collection. The help of Dr. A. Riccio, G. Sorrentino, and M. Amendola is also acknowledged.

Supporting Information Available: Experimental details. This material is available free of charge via the Internet at <http://pubs.acs.org>.

JA803363P

- (53) Safo, M. K.; Burnett, J. C.; Musayev, F. N.; Nokuri, S.; Abraham, D. J. *Acta Crystallogr., Sect. D: Biol. Crystallogr.* **2002**, *58*, 2031–2037.
- (54) Paoli, M.; Liddington, R.; Tame, J.; Wilkinson, A.; Dodson, G. *J. Mol. Biol.* **1996**, *256*, 775–792.
- (55) Paoli, M.; Dodson, G.; Liddington, R. C.; Wilkinson, A. J. *J. Mol. Biol.* **1997**, *271*, 161–167.
- (56) Park, S. Y.; Shibayama, N.; Hiraki, T.; Tame, J. R. *Biochemistry* **2004**, *43*, 8711–8717.
- (57) Shibayama, N.; Miura, S.; Tame, J. R.; Yonetani, T.; Park, S. Y. *J. Biol. Chem.* **2002**, *277*, 38791–38796.
- (58) Luisi, B.; Liddington, B.; Fermi, G.; Shibayama, N. *J. Mol. Biol.* **1990**, *214*, 7–14.